Cell

Adult c-kit^{pos} Cardiac Stem Cells Are Necessary and Sufficient for Functional Cardiac Regeneration and Repair

Georgina M. Ellison,[1,2,5,6,13] Carla Vicinanza,[1,2] Andrew J. Smith,[5,6] Iolanda Aquila,[2] Angelo Leone,[2] Cheryl D. Waring,[1] Beverley J. Henning,[1] Giuliano Giuseppe Stirparo,[7] Roberto Papait,[7,8] Marzia Scarfò,[9] Valter Agosti,[3,4] Giuseppe Viglietto,[3,4,9] Gianluigi Condorelli,[7,8,10] Ciro Indolfi,[2] Sergio Ottolenghi,[11] Daniele Torella,[1,2,12,*] and Bernardo Nadal-Ginard[1,5,6,12,13,*]

[1]Stem Cell and Regenerative Biology Unit (BioStem), Liverpool John Moores University, Liverpool L3 3AF, UK
[2]Laboratory of Molecular and Cellular Cardiology, Department of Medical and Surgical Sciences
[3]Laboratory of Molecular Oncology, Department of Experimental and Clinical Medicine
[4]CIS for Genomics and Molecular Pathology
Magna Graecia University, Catanzaro 88100, Italy
[5]Centre of Human and Aerospace Physiological Sciences, School of Biomedical Sciences
[6]Centre for Stem Cells and Regenerative Medicine
King's College, London, Guy's Campus, London SE1 1UL, UK
[7]Humanitas Clinical and Research Center, Rozzano-Milan 20098, Italy
[8]Institute of Genetics and Biomedical Research, National Research Council of Italy (CNR), Rozzano-Milan 20098, Italy
[9]IRGS-Biogem, Ariano Irpino, Avellino 83031, Italy
[10]University of Milan, Milan 20098, Italy
[11]Department of Biotechnology and Bioscience, University of Milano-Bicocca, Milan 20126, Italy
[12]These authors contributed equally to this work and are co-senior authors
[13]Present address: Centre of Human and Aerospace Physiological Sciences and Centre for Stem Cells and Regenerative Medicine, School of Biomedical Sciences, King's College, London, Guy's Campus, London SE1 1UL, UK
*Correspondence: dtorella@unicz.it (D.T.), bernardo.nadalginard@kcl.ac.uk (B.N.-G.)
http://dx.doi.org/10.1016/j.cell.2013.07.039

SUMMARY

The epidemic of heart failure has stimulated interest in understanding cardiac regeneration. Evidence has been reported supporting regeneration via transplantation of multiple cell types, as well as replication of postmitotic cardiomyocytes. In addition, the adult myocardium harbors endogenous c-kit^{pos} cardiac stem cells (eCSCs), whose relevance for regeneration is controversial. Here, using different rodent models of diffuse myocardial damage causing acute heart failure, we show that eCSCs restore cardiac function by regenerating lost cardiomyocytes. Ablation of the eCSC abolishes regeneration and functional recovery. The regenerative process is completely restored by replacing the ablated eCSCs with the progeny of one eCSC. eCSCs recovered from the host and recloned retain their regenerative potential in vivo and in vitro. After regeneration, selective suicide of these exogenous CSCs and their progeny abolishes regeneration, severely impairing ventricular performance. These data show that c-kit^{pos} eCSCs are necessary and sufficient for the regeneration and repair of myocardial damage.

INTRODUCTION

Most mammalian adult tissues harbor a subpopulation of tissue-specific stem and progenitor cells (hereafter referred together as stem cells) that differentiate into some or all of the parenchymal cells of their tissue of origin (Weissman, 2000). Cardiac resident stem cells in embryonic, neonatal, and adult mammalian heart have been identified by different membrane markers (c-kit, Sca-1, Abcg-2, Flk-1, and PDGFR-α) and transcription factors (Isl-1, Nkx2.5, GATA4, and Wt-1) (Vincent and Buckingham, 2010; Torella et al., 2007; Chong et al., 2011; Smart et al., 2011). It is likely that a number of these identified cell populations represent different developmental and/or physiological stages of a unique resident stem cell (Ellison et al., 2010).

Intensive research on the adult mammalian heart's capacity for self-renewal has led to a consensus that new cardiomyocytes (hereinafter CMs) are indeed formed throughout adult mammalian life (Hsieh et al., 2007; Bergmann et al., 2009). However, the physiological significance of this renewal, the origin of the new CMs, and the rate of adult CM turnover are still highly debated. Whereas some recent studies have calculated a yearly CM turnover of about 1% (Bergmann et al., 2009), others have calculated 4%–10% (Senyo et al., 2013) and some as high as 40% per year (Kajstura et al., 2012). Similar discrepancy exists regarding the origin of the new CMs and their physiological significance. Myocyte replacement, particularly after injury, was originally attributed to differentiation of a stem cell compartment

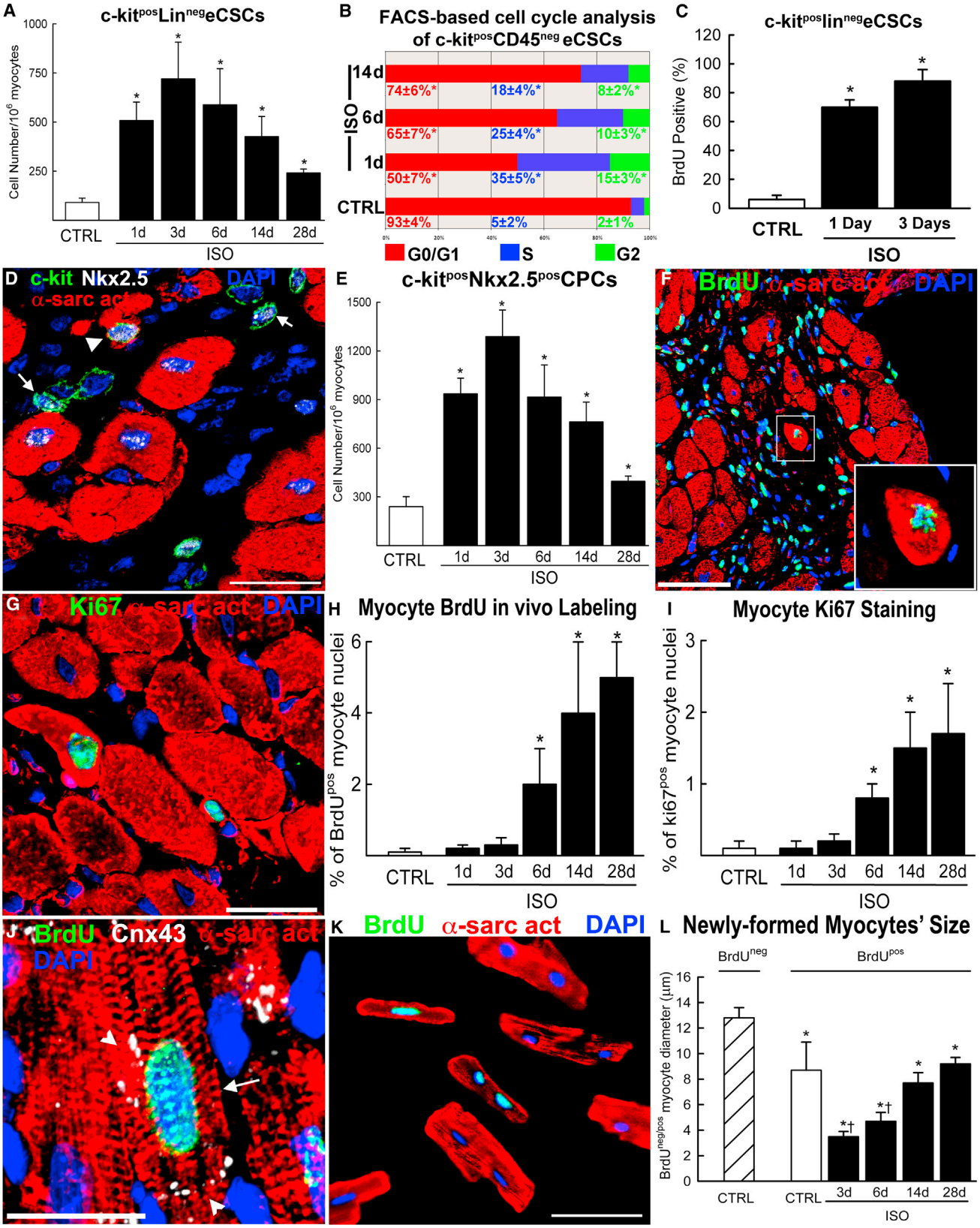

(legend on next page)

(Beltrami et al., 2003), a source confirmed by genetic cell fate mapping (Hsieh et al., 2007). More recently, it has been reported that CMs in the border zone of an infarct are replaced by the division of pre-existing postmitotic myocytes (Senyo et al., 2013). These results would shift the target of regenerative therapy toward boosting mature CM cell-cycle re-entry. However, the experiments of Senyo et al. (2013) document that a very small fraction of CM DNA replication occurs in cells that have already activated the myosin heavy chain (MHC) gene, a well-known aspect of myocyte development; these data fall short of documenting mature myocyte re-entry into the cell cycle.

The adult endogenous c-kit^{pos}CD45^{neg}tryptase^{neg} cardiac stem cells (hereafter, c-kit^{pos}eCSCs or just eCSCs) participate in adaptations to myocardial stress (Ellison et al., 2007a; Waring et al., 2012), and, when transplanted into the myocardium, regenerate most cardiomyocytes and microvasculature lost in an infarct (Beltrami et al., 2003). Recently, the in situ myogenic potential of adult c-kit^{pos} cardiac cells has been questioned as being significantly reduced, particularly in comparison to their neonatal counterparts (Zaruba et al., 2010; Jesty et al., 2012).

To revisit the regenerative potential of c-kit^{pos} eCSCs, we employed experimental protocols of severe diffuse myocardial damage which, unlike an experimental infarct, spares the eCSCs (Ellison et al., 2007b), in combination with several genetic murine models and cell transplantation approaches. Here, we demonstrated that eCSCs are necessary and sufficient for myocyte regeneration, leading to complete cellular, anatomical, and functional myocardial recovery.

RESULTS

Robust eCSC Activation and Myocyte Regeneration Follow Myocardial Damage in the Presence of a Patent Coronary Circulation

To follow c-kit^{pos}eCSC physiological response to cardiac injury, we induced severe diffuse myocardial damage in adult rats with a single high dose of isoproterenol (ISO) (Ellison et al., 2007b). New cell formation was monitored with bromodeoxyuridine (BrdU) labeling in vivo (Waring et al., 2012). In the presence of a patent coronary circulation, ISO produces a Takotsubo-like cardiomyopathy (Akashi et al., 2008) with both diffuse subendocardial and apical CM death. This acute insult kills 8%–10% of the left ventricle (LV) CMs and results in overt acute heart failure (Ellison et al., 2007b). Interestingly, the myocardial damage and heart failure spontaneously reverse anatomically and functionally by 28 days (Figure S1 available online). Whereas in the normal myocardium (CTRL) most c-kit^{pos}eCSCs are quiescent (>90% BrdU^{neg} and Ki67^{neg}), after ISO damage, a high fraction enters the cell cycle (Figures 1A–1C and S1). At day 3, ~88% are BrdU^{pos} (Figure 1C), leading to an ~8-fold increase in eCSC number, which decreases thereafter but remains above CTRL for up to 28 days (Figure 1A).

The expansion of the eCSC pool in response to CM loss by ISO damage was followed by their commitment to myocardial cell lineages. Indeed, many of the c-kit^{pos} eCSCs expressed GATA4 (Figure S1) and Nkx2.5 (Figures 1D and 1E), two early transcription factors of the cardiac lineage which, together with Tbx5 and MEF-2C, are essential for the differentiation of mesoderm and reprogramming of fibroblasts into the CM lineage (Takeuchi and Bruneau, 2009; Qian et al., 2012; Song et al., 2012). The number of c-kit^{pos}Nkx2.5^{pos}GATA4^{pos} cells increased ~4-fold over CTRL by day 3 (Figures 1E and S1). This sequential transition from undifferentiated cells to committed progeny is further illustrated by the transcription of sarcomeric and gap junction genes (troponin I, *cTnI*; connexin 43, *Cnx43*) and the presence of their corresponding proteins, even though at lower levels than found in the adult spared CMs (Figures 1D and S1). These new c-kit^{pos}GATA-4^{pos}Nkx2.5^{pos} myogenic progenitors express β-MHC, the isoform characteristic of the fetal rat heart (Lompré et al., 1984). No expression of the α-*Mhc* gene, characteristic of adult rat CMs and expressed by spared CMs 72 hr after ISO, was detected (Figure S1).

Starting at day 3 post-ISO, very small mononucleated BrdU^{pos}Ki67^{pos} CMs, including some in mitosis, were detected (Figures 1F–1L), which is indicative of immature, proliferative CMs. These new CMs were localized mainly in the LV subendocardium and apex, the area most severely damaged by ISO. From 3 to 28 days, there was a significant increase in the number (Figures 1H and 1I) and size of these CMs, which were nearly all mononucleated and smaller than the spared (BrdU^{neg}) ones (Figure 1L). The BrdU^{pos} CMs also expressed CNX43, suggestive of gap junction formation and integration with the neighboring myocardium (Figure 1J). Rod-shaped small BrdU^{pos} CMs were also detected as single cells when isolated from ISO-treated hearts (Figure 1K). Their smaller size indicates that, despite the normal histology and function of the ISO-treated hearts 4 weeks postinjury, the newly regenerated CMs had not yet fully matured.

Myocyte Regeneration after Diffuse Myocardial Damage Is Not the Product of Pre-existing Myocyte Division or Bone Marrow Cells

BrdU labeling and Ki67 expression cannot establish whether the new CMs are generated by the reported division of pre-existing

Figure 1. eCSC Activation and Myogenic Differentiation following Diffuse Myocardial Damage

(A–C) c-kit^{pos}eCSCs in myocardium (A), FACS cell-cycle analysis (B), and percentage of activated c-kit^{pos}BrdU^{pos}eCSCs (C) in CTRL and after ISO. *$p < 0.01$ versus CTRL.

(D and E) Confocal microscopy (D) and quantification of c-kit^{pos}/Nkx2.5^{pos} progenitors (E; arrows) and myogenic precursor (arrowhead) 3 days after ISO. Scale bar, 20 μm. *$p < 0.01$ versus CTRL.

(F–I) Confocal microscopy (F and G) and quantification (H and I) of small newly formed (BrdU) mitotic and proliferating (Ki67) CMs 28 days after ISO. 50 mg kg^{-1} of BrdU was injected (i.p.) twice daily. Scale bar, 50 μm (F) and 20 μm (G). *$p < 0.05$ versus CTRL.

(J) Confocal microscopy of a small BrdU^{pos} CM (arrow) with gap junction formation (Cnx43, white; arrowheads) between neighboring CMs 28 days after ISO. Scale bar, 20 μm.

(K) Rod-shaped BrdU^{pos} ventricular CMs isolated 28 days after ISO (n = 4). Scale bar, 50 μm.

(L) BrdU^{pos} CM diameter. *$p < 0.05$ versus CTRL BrdU^{neg}; †$p < 0.05$ versus CTRL BrdU^{pos}.

All data are mean ± SD. See also Figure S1.

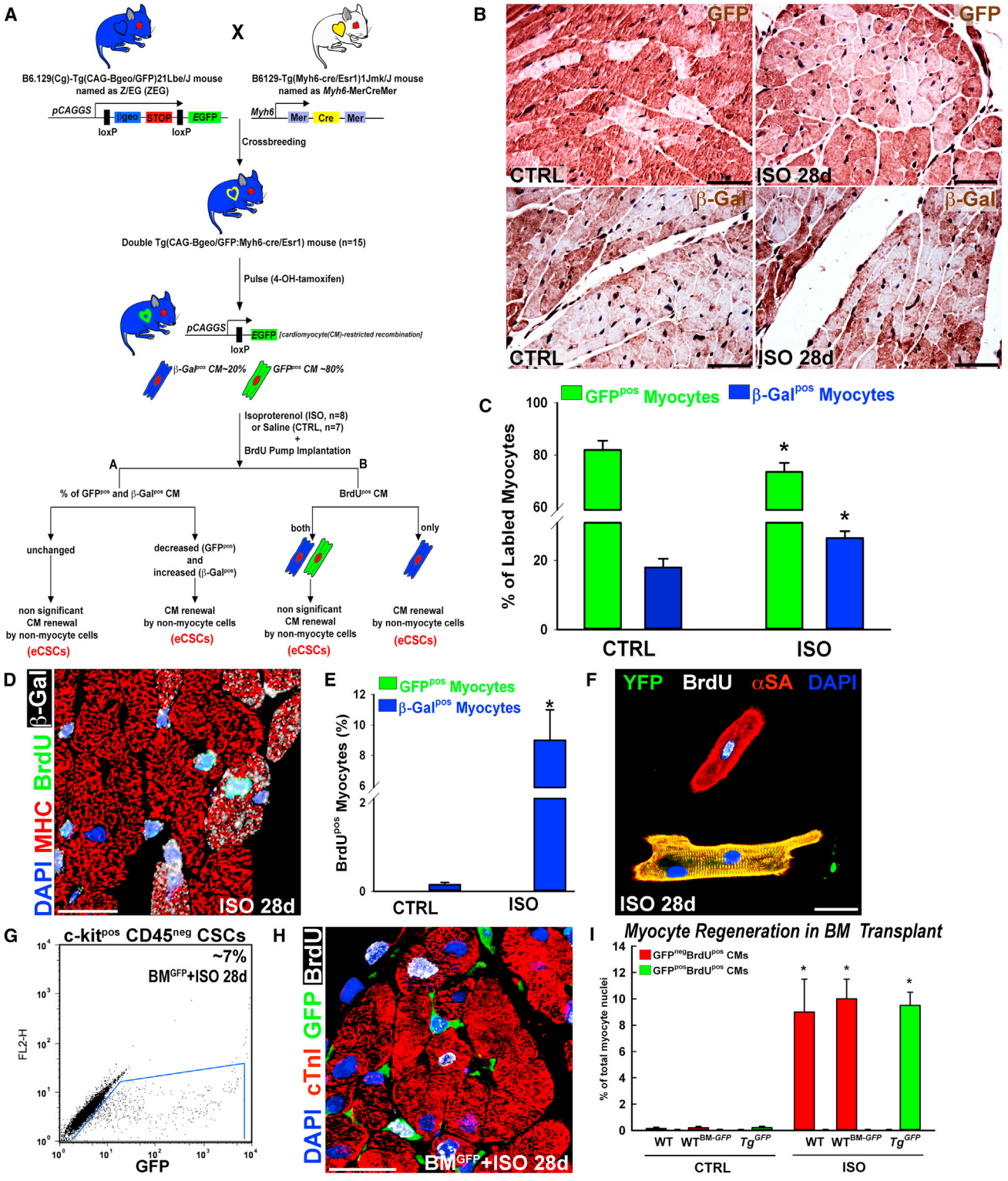

Figure 2. Myocyte Regeneration after Diffuse Myocardial Damage

(A) Schematic of pulse-chase genetic labeling of CM renewal.

(B) Representative immunostaining with antibodies against GFP and β-gal (both brown-DAB staining) in the subendocardial, apical layer of CTRL 28 days after ISO. Scale bar, 50 μm.

(C) Fraction of GFP^{pos} and β-gal^{pos} CMs in CTRL and after ISO. *$p < 0.05$ versus CTRL.

(legend continued on next page)

adult CMs or by the activation and ensuing differentiation of a stem cell compartment. To specifically address this issue, we traced the cell lineage of the new CMs. We generated double-transgenic mice (MerCreMer-ZEG) (Hsieh et al., 2007; Loffredo et al., 2011) in which, upon tamoxifen administration, β-galactosidase (β-gal) is replaced by enhanced GFP exclusively in cardiac cells that have already activated the *Myh6* gene (and, therefore, the transgene carrying the cre recombinase gene), which are either postmitotic CMs or amplifying cells already committed to the CM lineage (i.e., immature myocytes/myocyte precursors).

In tamoxifen-naive MerCreMer-ZEG mice, 99 ± 0.2% of the CMs express β-gal and are negative for GFP (the leakage of the Myh6-Cre construct in these animals is ~0.2%). Tamoxifen correctly switched β-gal to GFP in CMs (Figures 2A–2C). This resulted in hearts composed of 83 ± 3% GFP^{pos} and 17 ± 2% $\beta\text{-gal}^{pos}$ CMs (Figures 2B and 2C), as previously reported (Hsieh et al., 2007; Senyo et al., 2013). In this setting, if new CMs ($BrdU^{pos}$) originated from division of pre-existing CMs, they should be mostly GFP^{pos}, and the ratio between GFP^{pos} and $\beta\text{-gal}^{pos}$ CMs should remain unchanged at ~80/20. If instead the new CMs originate from non-CM cells, they should be $\beta\text{-gal}^{pos}$ and produce a "dilution" of GFP^{pos} CMs with a decrease of the $GFP^{pos}/\beta\text{-gal}^{pos}$ CM ratio (Figure 2A).

In mice, ISO injection caused the same type of myocardial damage and LV dysfunction shown in rats, resulting in $c\text{-kit}^{pos}$ eCSC activation, CM regeneration, and recovery of cardiac function (Figure S2). When ISO was administered to CM-recombined MerCreMer/ZEG mice (Figure 2A) followed by BrdU labeling, 28 days later there was a significant increase in the percentage of $\beta\text{-gal}^{pos}$ CMs: 18% ± 2.5% in saline-treated mice versus 26.5 ± 2% in ISO-injured mice (Figures 2B and 2C), accompanied by a decrease of GFP^{pos} CMs in the hearts of ISO-treated mice (73.5 ± 3.5%) compared to CTRL mice (82 ± 3.5%) (Figures 2B and 2C). There was also a concomitant increase of $BrdU^{pos}$ CMs (9 ± 2%) in the ISO-treated hearts, and these were $\beta\text{-gal}^{pos}$ (Figures 2D and 2E). These numbers match the CM loss produced by ISO administration (Figure S2). In contrast, we detected very few newly generated $BrdU^{pos}\beta\text{-gal}^{pos}$ CMs (0.15 ± 0.05%) in saline-treated CTRL mice (Figure 2E). This result concurs with Hsieh et al. (2007) but disagrees with the interpretation of Senyo et al. (2013) using the same genetic tools. This discrepancy might be due to the different injury models used. In contrast to coronary ligation, ISO kills a large number of CMs in the presence of patent coronary circulation, and it spares the eCSCs. Thus, ISO provides a more physiologic test for the endogenous reparative potential of the adult heart (Ellison et al., 2007b). Furthermore, during the 2 week administration of tamoxifen for Cre induction, it would be expected that some eCSCs have committed to the myogenic lineage and activated the *Myh6* gene with recombination of the transgene and generation of $\beta\text{-gal}^{pos}$ CMs, as reported by Dong et al. (2012).

Although cell fusion might allow the expression of both GFP and β-gal in the same CM, it can be ruled out because the percentage of CMs positive for both markers was negligible (<0.1%) in saline-treated CTRL and ISO-injured mice. The possibility that the decrease in GFP^{pos} and corresponding increase in $\beta\text{-gal}^{pos}$ CMs after ISO might be due to a higher susceptibility of GFP-labeled CMs to ISO damage was also excluded by the fact that the percentage of necrotic and apoptotic GFP^{pos} and $\beta\text{-gal}^{pos}$ CMs 1 day after ISO was similar (Figure S2).

Finally, we dissociated to single cells CMs from the hearts of double-transgenic MerCreMer:RYP mice obtained by crossing MerCreMer with R26R-EYFP (RYP) mice (Qian et al., 2012), in which the CMs were labeled with the enhanced yellow fluorescent protein (EYFP) upon tamoxifen injection. In agreement with the data shown on MerCreMer:ZEG mice, tamoxifen-driven induction of YFP marked ~80% of endogenous CMs in the uninjured CTRL heart, which decreased to ~72% in the apex (and subendocardium) of injured hearts at 28 days after ISO. Only the YFP^{neg} fraction isolated from the CM-recombined double-transgenic mice was $BrdU^{pos}$ (Figure 2F). Most of these newly generated $BrdU^{pos}YFP^{neg}$ CMs were rod shaped, mononucleated, and smaller than the pre-existing (mostly binucleated) $YFP^{pos}BrdU^{neg}$ CMs (Figure 2F).

In conclusion, after diffuse myocardial injury, new CMs are not generated (at least in quantities above background) through the division of pre-existing terminally differentiated CMs as claimed (Senyo et al., 2013) but rather are generated from non-CM cells with the characteristics of a stem compartment (Hsieh et al., 2007).

Bone marrow (BM)-derived cells have been implicated in cardiac regeneration after myocardial infarction (Orlic et al., 2001; Loffredo et al., 2011). To test this possibility, either saline or ISO was injected to sublethally γ-irradiated mice 3 months after successful reconstitution of their BM with BM cells from Tg^{GFP} mice (Sata et al., 2002). In both CTRL and ISO-treated animals, a small fraction (3.5 ± 2% versus 5 ± 2%, respectively) of $c\text{-kit}^{pos}CD45^{neg}$ cardiac cells was GFP positive at 28 days (Figure 2G). However, despite extensive histological analysis and CM isolation, we were unable to find a single BM-derived $GFP^{pos}BrdU^{pos}$ or GFP^{pos} CM in either ISO-treated or CTRL hearts (Figures 2H and 2I). Therefore, BM-derived cells do not directly contribute in any significant manner to new CM formation in normal or ISO-damaged hearts.

New Myocytes after Diffuse Myocardial Injury Originate from Resident $c\text{-kit}^{pos}$eCSCs

To determine whether $c\text{-kit}^{pos}$eCSCs replenish the CMs lost by diffuse myocardial damage, we genetically tagged in situ a

(D and E) Confocal microscopy (D) and percentage (E) of newly formed $\beta\text{-gal}^{pos}/BrdU^{pos}$ CMs 28 days after ISO. Scale bar, 20 μm. *$p < 0.05$ versus CTRL.
(F) Immunocytochemistry identifies a small $BrdU^{pos}/YFP^{neg}$ mononucleated rod-shaped CM, isolated from pulse-labeled MerCreMer:RYP mice, 28 days after ISO.
(G) Flow cytometric analysis of GFP within the $c\text{-kit}^{pos}/CD45^{neg}$ eCSC compartment, following BM^{GFP} transplantation and 28 days after ISO. n = 5.
(H) Confocal microscopy of newly formed $BrdU^{pos}/GFP^{neg}$ CMs.
(I) CM regeneration after BM^{GFP} transplantation. *$p < 0.05$ versus CTRL.
All data are mean ± SD. See also Figure S2.

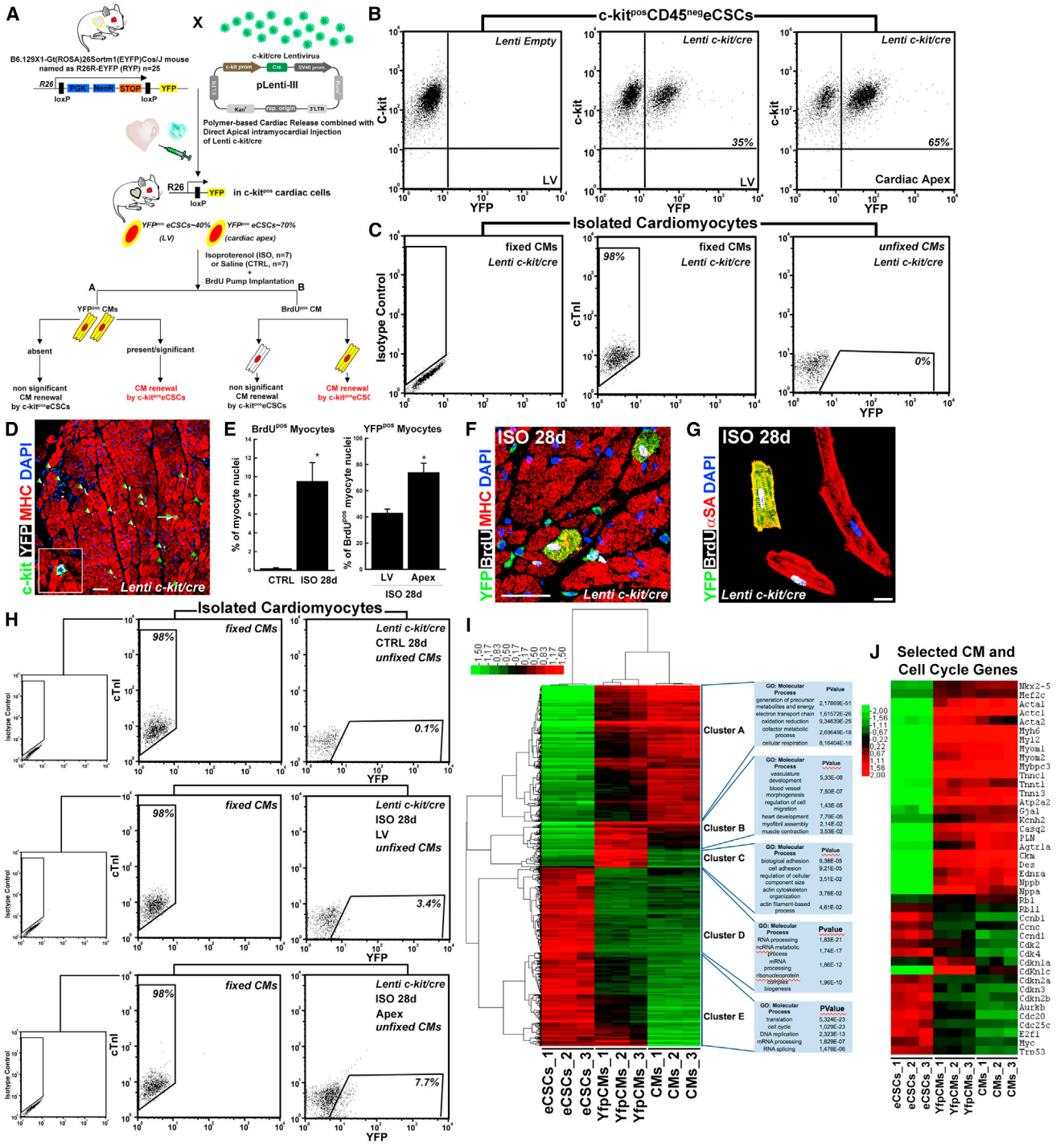

Figure 3. Myocyte Replenishment by c-kit^{pos} eCSCs following Diffuse Myocardial Damage

(A) Schematic of pulse-chase genetic labeling approach of resident c-kit^{pos}eCSCs and their progeny in situ.

(B and C) Flow cytometric analysis shows c-kit/cre lentivirus labeling of eCSCs and CMs in vivo.

(D) Representative confocal microscopy of apical YFP-labeled c-kit^{pos}eCSCs (c-kit/YFP, green/white arrowheads; c-kit^{pos} eCSCs not transfected, green arrowheads). Scale bar, 20 μm.

(E) Percentage of BrdU^{pos} CMs and those that were YFP^{pos} in the LV and apex 28 days after ISO. Data are mean ± SD. *$p < 0.05$ versus CTRL or LV.

(F) Representative confocal microscopy of apical c-kit^{pos}eCSC-derived YFP^{pos}BrdU^{pos} CMs 28 days after ISO. Scale bar, 20 μm.

(G and H) Representative immunocytochemistry of BrdU^{pos}/YFP^{pos} and BrdU^{pos}/YFP^{neg} isolated CMs (G) and flow cytometric analysis of YFP/cTnI^{pos} CMs (H) isolated from lenti c-kit/cre mice 28 days after ISO or saline (CTRL). n = 3.

(legend continued on next page)

subset of adult resident c-kit^{pos}eCSCs and their myocyte committed progeny (Figure 3A). We generated a lentivirus carrying Cre-recombinase under the control of the c-kit promoter (Lenti-c-kit/Cre) with a pattern of expression restricted to c-kit^{pos} cells (Figure S3; Cairns et al., 2003). To confine lentivirus release to the LV myocardium, we employed a fibrin-based PEGylated hydrogel for epicardial delivery (Zhang et al., 2006). To increase delivery, we also injected the lentivirus directly into the apex, the region with the greatest CM damage after ISO (Ellison et al., 2007b) and with the highest concentration of c-kit^{pos} eCSCs (Ellison et al., 2011). This combined strategy was used to selectively release Lenti-c-kit/Cre into the myocardium of RYP reporter mice (Figure 3A). In these mice, the uptake of the c-kit/Cre recombinase lentivirus by any c-kit^{pos} cell deletes the STOP sequence in the transgene and switches on the expression of EYFP. After 2 weeks, peripheral blood cells and BM-derived cells were reproducibly negative for EYFP (Figure S3). Importantly, 38 ± 5% of total and 65 ± 7% of apex-confined c-kit^{pos}eCSCs were EYFP positive (Figures 3B–3D). Lenti-c-kit/Cre injection induced EYFP expression exclusively in cardiac c-kit^{pos} cells, whereas CMs (Figure 3C) and other c-kit^{neg} myocardial cell types were all negative for EYFP (Figure S3). When the recombined EYFP^{pos}c-kit^{pos}CD45^{neg}eCSCs were isolated from the hearts of RYP mice at 2 weeks after lentivirus release, they were phenotypically indistinguishable from the unrecombined EYFP^{neg}-c-kit^{pos}CD45^{neg}eCSCs and exhibited the typical properties of resident eCSCs, being clonogenic, self-renewing, and multipotent (Figure S3).

14 days after local release of the Lenti-c-kit/Cre, RYP mice received either ISO or saline (CTRL) injection. 28 days after ISO, we confirmed that there were no recombined EYFP-positive cells in the c-kit^{pos}-enriched fraction of the nucleated cells of peripheral blood or within the BM from CTRL and ISO-injured mice (Figure S3). In CTRL mice, after 4 weeks of BrdU in vivo labeling, a total of 0.18 ± 0.07% BrdU^{pos} CMs was detected, and only a fraction of those newly generated cells were c-kit^{pos} eCSC-derived EYFP^{pos}BrdU^{pos} CMs (0.06 ± 0.02%/total CMs) (Figure 3E). In the ISO-treated hearts, a significant fraction of a total 9.5 ± 2% of newly formed CMs were EYFP positive (43 ± 3% of total BrdU^{pos} CMs, which, in the apex, reached 74 ± 7%) (Figures 3E and 3F), indicating that these newly generated CMs are the progeny of the c-kit^{pos}eCSCs. We confirmed the identity of both YFP^{pos}- and YFP^{neg}-BrdU^{pos} CMs in isolated CMs 28 days after ISO (Figure 3G) by fluorescence-activated cell sorting (FACS). YFP expression was analyzed in unfixed CMs to avoid fluorescent protein leakage, as well as fixative-induced autofluorescence. FACS detected >98% cTnI-positive cells in the fixed aliquot of the CM preparation in both CTRL and ISO groups (Figure 3H). <0.5% of YFP^{pos} cells were detected in the unfixed aliquot of the same CM preparation from CTRL c-kit/Cre recombined RYP mice (Figure 3H). Thus, it was technically impossible to ascertain by FACS whether they were truly c-kit^{pos} eCSC-derived CMs. More significantly, YFP^{pos} cells were clearly recognized within the unfixed CM preparation from ISO-injured hearts (2.9 ± 0.5% in total LV and 8.3 ± 1% in LV apex) (Figure 3H). We further verified that the YFP signal truly originated from YFP^{pos} CMs by sorting the total CM preparation and demonstrating that ≥99% were αSA positive after cell fixation (Figure S4). These results were not due to c-kit re-expression in adult CMs, as suggested previously in cryo-injured hearts (Tallini et al., 2009). The absence of such re-expression in saline- or ISO-treated transgenic mice expressing GFP under the c-kit promoter (Figure S4) rules out this potential confounding factor.

To further test the identity and the degree of differentiation of the newly regenerated eCSC-derived CMs, we obtained global gene expression profiles by microarray of c-kit^{pos} eCSCs, c-kit^{pos} eCSC-derived YFP^{pos} CMs, and normal adult CMs. The c-kit^{pos} eCSC-derived YFP^{pos} CMs were obtained by FACS sorting from Lenti-c-kit/cre recombined RYP mice 28 days after ISO injury (Figure S4). These CMs had a gene expression profile that closely resembled the profile of adult CMs (Figures 3I and 3J). Comparison of c-kit^{pos}eCSCs versus c-kit^{pos}CSC-derived YFP^{pos} CMs versus adult mature CMs reveals a clear transcriptome shift going from uncommitted c-kit^{pos}CSCs to CM-lineage commitment, followed by immature to mature CMs (Figures 3I and 3J and Table S1). The eCSC-derived YFP^{pos} CMs expressed the main CM transcription factors, as well as sarcomeric contractile genes, but still maintained the expression of cell-cycle-related and high-metabolic-state genes typical of immature (neonatal) not yet terminally differentiated CMs (Figures 3I and 3J). Intriguingly, even after having acquired mature sarcomeric structures and a rod shape (Figure 3G), eCSC-derived YFP^{pos} CMs show an incomplete switch from retinoblastoma-like 1 (*Rbl-1* or *p107*) to retinoblastoma protein (*Rb*), which is a requirement for permanent CM withdrawal from the cell cycle (Schneider et al., 1994). These data further demonstrate that resident c-kit^{pos}eCSCs generate new CMs in vivo that are still immature 4 weeks after their birth.

Taken together, these in vivo genetic cell-fate-mapping experiments show that c-kit^{pos}eCSCs have intrinsic cardiac regenerative potential, replacing lost CMs lost after diffuse myocardial injury.

c-kit^{pos}eCSCs Have Strong Tropism for the Damaged Myocardium

To determine whether the ISO-injured myocardium provides a homing milieu for c-kit^{pos}eCSCs, 5 × 10^5 cells derived from a single eCSC GFP-tagged clone (eCSCs^{GFP}) (Figure 4A) were injected through the tail vein of rats 12 hr after ISO injury. As cell control, ISO-injured rats were injected with 5 × 10^5 GFP-tagged c-kit negative sorted CM-depleted cardiac cells (c-kit^{neg}MDCCs^{GFP}; containing 86 ± 5% cardiac fibroblasts, 13 ± 3% vascular smooth muscle, 1 ± 1% endothelial and <0.001% c-kit^{pos} cardiac cells). To control for the role of injury in the

(I) Heatmap showing two-way hierarchical cluster of the expression of 3,774 genes that underwent a log fold change ≥ 1 or ≤ −1 ($p < 0.005$). See also Table S1. Enriched Gene Ontology (GO) terms for the genes of each cluster are shown to the right.

(J) Heatmap showing expression pattern of CM and cell-cycle-specific genes in c-kit^{pos}eCSCs, YFP^{pos} CMs, and adult terminally differentiated CMs. n = 3 for each.

See also Figures S3 and S4 and Table S1.

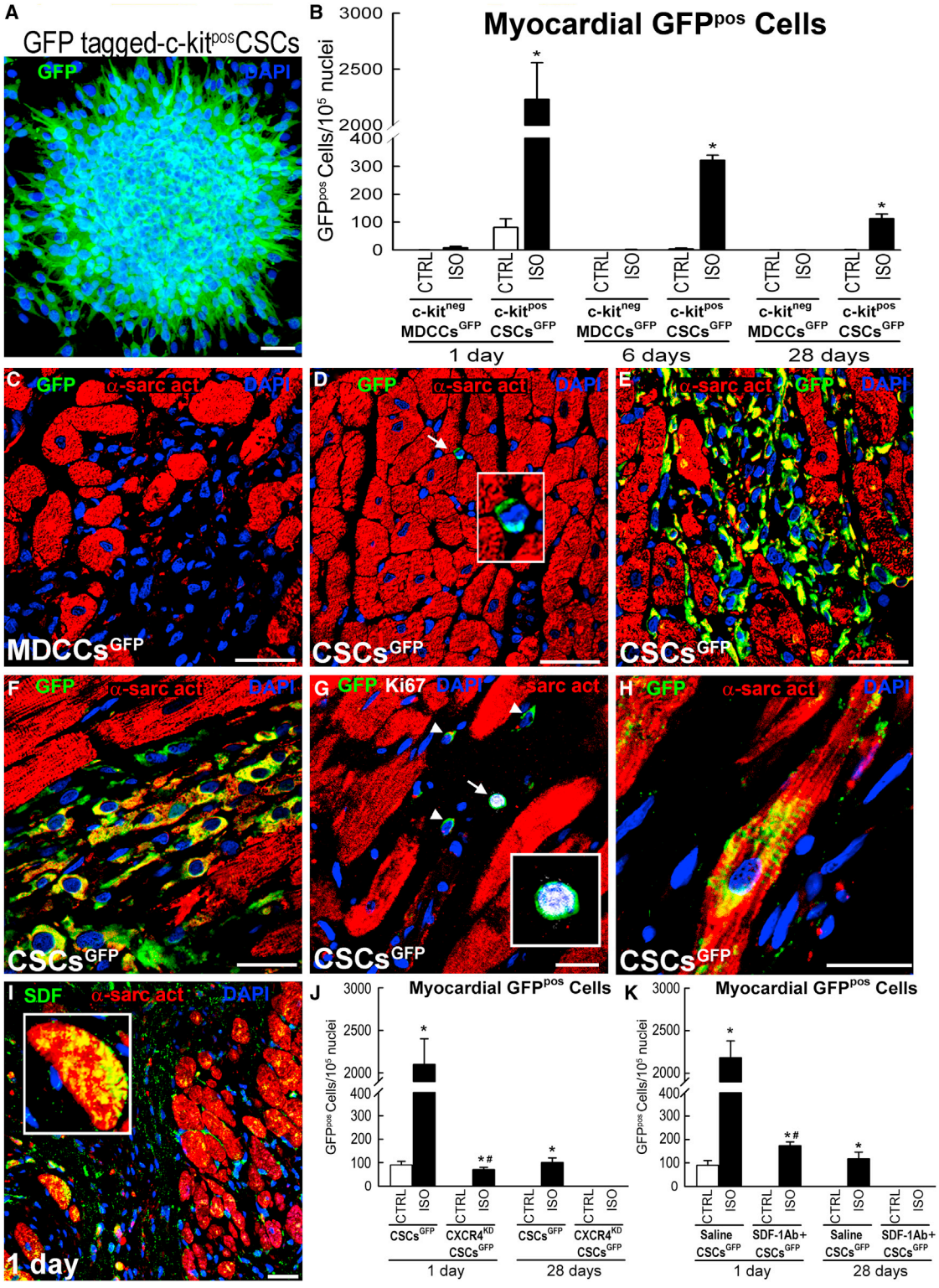

Figure 4. c-kit^{pos}CSCs Exhibit Selective Homing to ISO-Damaged Myocardium and Differentiate into New CMs

(A) Immunocytochemistry of clonal c-kit^{pos}CSCs^{GFP}. Scale bar, 50 μm.

(B) Quantification of tail-vein-injected c-kit^{neg}MDCCs^{GFP} and c-kit^{pos}CSCs^{GFP} in the subendocardial layer after ISO. *$p < 0.001$ versus CTRL and c-kit^{neg} MDCCs^{GFP}.

(C–F) Confocal microscopy representative images of GFP^{pos} c-kit^{neg}MDCCs (C) and c-kit^{pos}CSC^{GFP} in the myocardium of CTRL (D) and at 1 (E) and 6 (F) days after ISO and tail-vein injection. Scale bar, 30 μm.

(legend continued on next page)

homing, both cell preparations were also administered to uninjured, saline-treated (CTRL) animals.

At all time points, the myocardium of CTRL and ISO animals transplanted with c-kit^{neg}MDCCs^{GFP} had on average <1 GFP^{pos} cell/10^5 nuclei (Figures 4B and 4C). In the CTRL hearts transplanted with CSCs^{GFP}, there were 81 ± 31 CSCs^{GFP}/10^5 nuclei at 24 hr after injection (Figures 4B and 4D and Table S2). In contrast, in ISO-injured hearts, there was very efficient cardiac homing and engrafting of the transplanted CSCs^{GFP}, which accounted for most of the injected cells (Figures 4B, 4E, and 4F) (Table S2). The high cardiac tropism and engrafting efficiency of the cloned CSCs^{GFP} compared to the extra-cardiac tissues is shown in Table S2 and Figure S5. Of the myocardial-homed CSCs^{GFP}, 55 ± 5%, 20 ± 4%, and 8 ± 3% were Ki67^{pos} at 1, 6, and 28 days posttransplantation, respectively (Figure 4G). There was also an increase in GFP^{pos} cells expressing α-sarcomeric actin at 6 (25 ± 3%) and 28 (42 ± 3%) days. At 28 days, CSC^{GFP}-derived newly formed GFP^{pos} CMs (4 ± 1%; Figure 4H) had well-developed sarcomeres and were larger and more differentiated (diameter of 10 ± 2μm) but were still smaller than normal adult fully differentiated GFP^{neg} CMs (diameter of 14 ± 1μm; $p < 0.01$ versus GFP^{pos} CMs). We further quantified the number of transplanted c-kit^{pos}CSC-derived GFP^{pos} CMs by FACS, which was in agreement with the immunohistochemistry data (Figure S5). At 28 days after ISO and CSC^{GFP} tail-vein injection, of the total GFP^{pos} cardiac cells, the majority became CMs (64 ± 4%) but also became smooth muscle (10 ± 3%) and endothelial (14 ± 3%) vascular cells and fibroblasts, whereas few of them stayed as c-kit^{pos}CSCs (Table S3).

To further ascertain that the tail-vein-injected cells generated bona fide CMs, c-kit^{pos}eCSCs expressing GFP under the control of the cardiac troponin I (cTnI) promoter were tail injected after ISO as above. At 28 days, a population of CSC-derived cTnI^{pos}GFP^{pos} CMs was detected (Figure S5).

Because the SDF-1-CXCR4 axis is involved in retention and mobilization of stem cells in the adult (Askari et al., 2003), we evaluated whether this receptor-ligand pair homes CSCs^{GFP} to ISO-injured myocardium. SDF-1 is rapidly upregulated in CMs after ISO damage (Figures 4I and S5). 5 ×10^5-c-kit^{pos}eCSCs genetically modified to knock down expression of the SDF-1 receptor with a lentiviral vector carrying a CXCR4 shRNA tagged with GFP (CXCR4^{KD}CSCs^{GFP}; Figure S5) were tail-vein injected into rats 12 hr after ISO injury. The CXCR4^{KD}CSCs^{GFP} did not show any cardiac tropism, as most were lodged in the spleen and lungs (Figure 4J and Table S4). Concurrently, tail-vein-injected CSCs^{GFP} also failed to home to the myocardium of ISO-injured rats treated with an anti-SDF-1 neutralizing antibody 20 min before and 12 hr after cell injection (Figure 4K).

These results show that the c-kit^{pos}CSCs have a strong tropism for the damaged myocardium, which is CXCR4-SDF-1 dependent and is where the enhanced expression of SDF-1 by the surviving myocardium serves as a positive chemotactic agent.

c-kit^{pos}eCSCs Are Necessary and Sufficient for Myocyte Regeneration and Functional Recovery after Severe Diffuse Myocardial Damage

To test whether c-kit^{pos}eCSCs are necessary and/or sufficient for myocardial anatomical and functional regeneration, 3 days after ISO, we eliminated the proliferating eCSCs and their progeny through administration of the antimitotic agent 5-flurouracil (5-FU; 10 mg kg^{-1}). This regime (ISO+5-FU) ablated eCSC expansion and new CM formation (Figures 5A–5C), resulting in a severe cardiomyopathy (ISO+5-FU induced) (Figure 5D) with a deficit and significant hypertrophy of the spared CMs, as compared to animals treated with ISO alone (ISO+saline), in which regeneration was normal (Figure S6). Although all ISO+saline animals survived the acute myocardial insult and fully recovered cardiac function, the ISO+5-FU animals developed heart failure (Figures 5D and S6) with increased mortality (4 of 10 ISO+5-FU-treated animals versus 0 of 10 for the ISO+saline animals) at 28 days. These effects were not due to 5-FU toxicity because the same 5-FU regime administered to control animals did not cause any cellular or functional cardiac or extracardiac toxic effects, including in the bone marrow (Figure S6). However, 5-FU would have targeted other replicating cells together with activated eCSCs. Indeed, at 3 days after ISO when 5-FU started to be administered, the eCSCs represented only 17 ± 3% of total Ki67-positive myocardial cells, whereas 55 ± 4% were inflammatory cells (i.e. granulocytes and macrophages). A small fraction was cycling cardiac fibroblasts (9 ± 2%), smooth muscle (4 ± 1%), and endothelial (5 ± 2%) cells.

To evaluate the effect, if any, of ablating non-eCSCs on blocking the regenerative response and simultaneously to establish a causal relationship between eCSC activation on one hand and myocardial regeneration and repair on the other, we injected 5 × 10^5 cloned CSCs^{GFP} or the same number of GFP^{pos} cardiac fibroblasts (cFibro) into the tail vein of rats with ISO+5-FU cardiomyopathy 28 days after ISO. Additionally, to address whether the transplanted cells and their progeny are continuously required to maintain cardiac cell homeostasis and functional recovery, in a separate set of animals, we transplanted cells from an eCSC clone expressing GFP together with the herpes simplex virus thymidine kinase (CSC$^{GFP/TK}$). Ganciclovir (GCV) administration produces selective suicide of the transplanted CSC$^{GFP/TK}$ and their progeny (Figure S7). As an additional control, saline was tail-vein injected into another group of animals. See Figure 6A for the study design.

At 2 months, the surviving rats with ISO+5-FU cardiomyopathy that received either saline or cFibro were indistinguishable and in overt heart failure with a dramatic deficit in c-kit^{pos}eCSCs, a lack of CM regeneration, and increased CM death and hypertrophy (Figures 6B, 6D, and S7). In contrast, 95% of the animals treated with CSCs^{GFP} were alive at 2 months, showing efficient homing and nesting of CSCs^{GFP} into the damaged myocardium, which had reconstituted the resident eCSC pool (~90% cell

(G and H) Confocal microscopy of a Ki67^{pos} (G; arrow) CSC^{GFP} (arrowheads) and a CSC^{GFP}-derived CM 28 days after ISO and tail-vein injection (H). Scale bar, 20 μm.
(I) Immunohistochemistry with antibody against SDF-1 (green; inset shows CM-specific expression) in the ISO-injured myocardium. Scale bar, 20 μm.
(J and K) Quantification of CXCR4^{KO}c-kit^{pos}CSCs^{GFP} (J) and c-kit^{pos}CSC^{GFP} in rats treated with a SDF-1-neutralizing antibody (SDF-1Ab) (K). *$p < 0.05$ versus CTRL. #$p < 0.05$ versus ISO 1 day.
All data are mean ± SD. See also Tables S2, S3, and S4 and Figure S5.

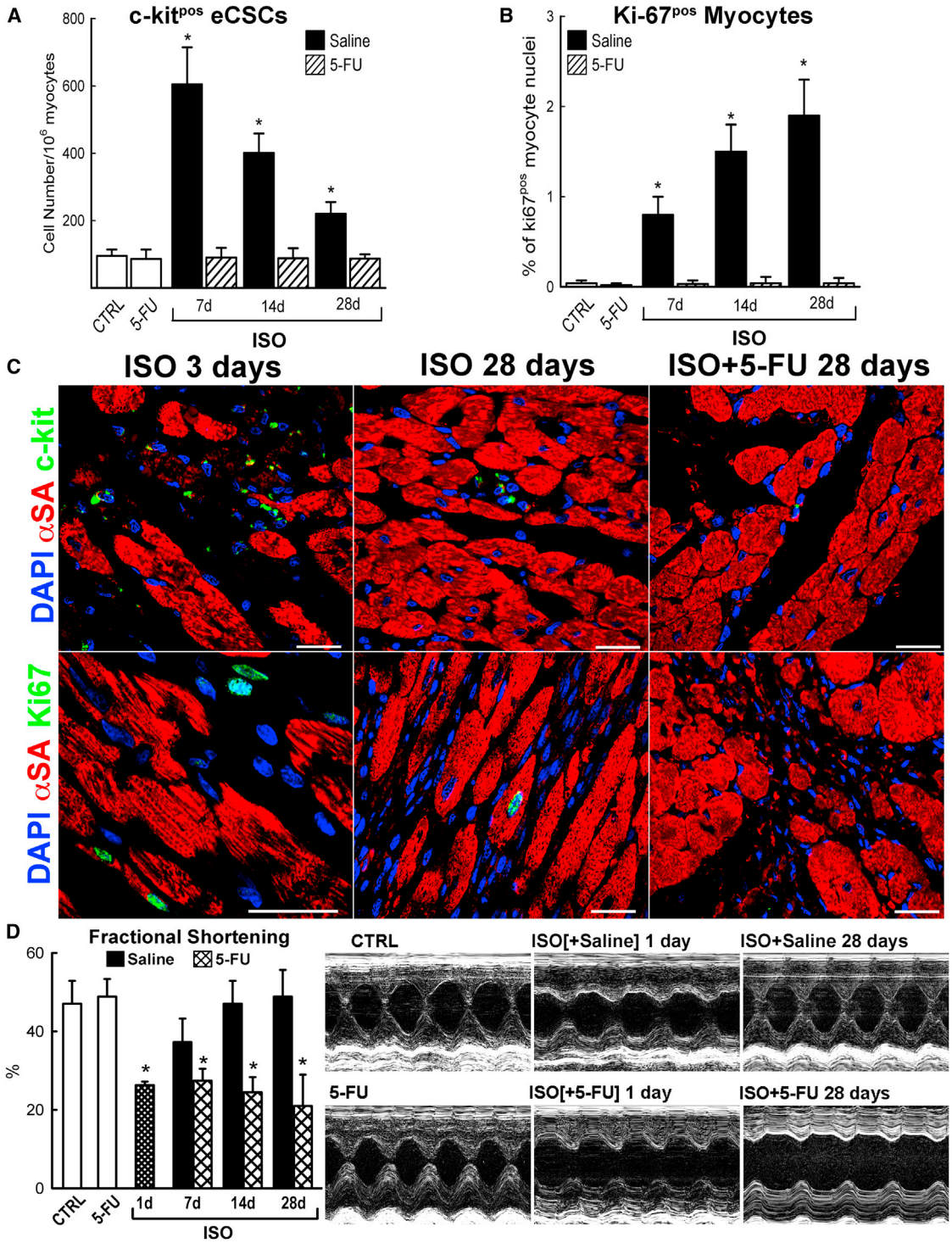

Figure 5. Ablation of c-kit^{pos} eCSCs Blocks Myocyte Regeneration

(A and B) Quantification of c-kit^{pos}eCSCs and Ki67^{pos} new CM formation after ISO+5-FU treatment. *$p < 0.01$ versus CTRL and 5-FU.

(C) Confocal microscopy representative immunostaining of c-kit and Ki67 on ISO+5-FU-treated LV sections compared to 3 and 28 days after ISO. Scale bar, 30 μm.

(D) Echocardiographic LV function measurements following ISO+5-FU administration compared to ISO+saline. *$p < 0.05$ versus CTRL and 5-FU.

All data are mean ± SD. See also Figure S6.

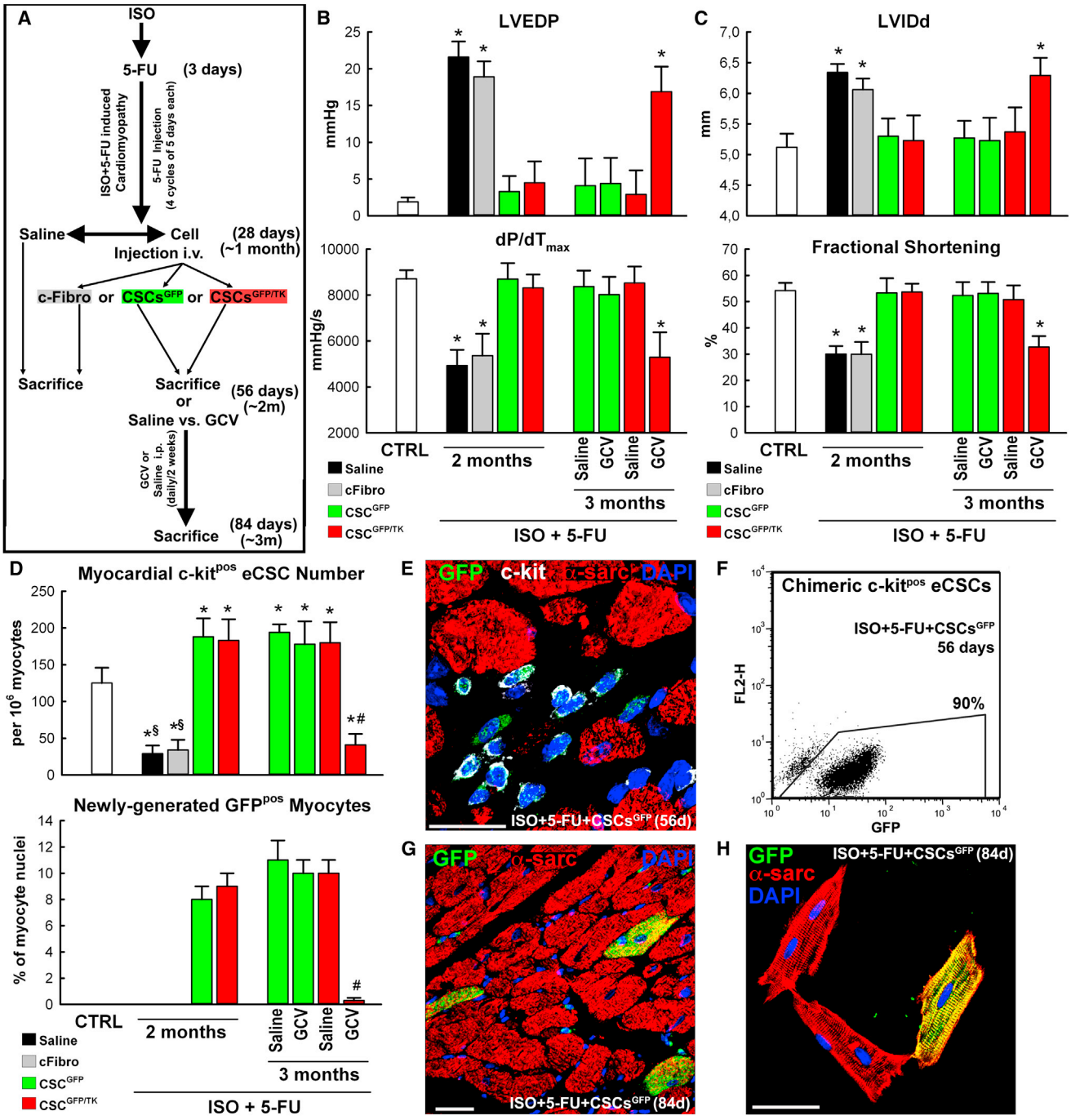

Figure 6. Restoration of the eCSC Pool through Exogenous c-kit^{pos} eCSC Transplantation Normalizes Myocardial Tissue Composition and Function

(A) Brief schematic of in vivo rat study design.

(B and C) Echocardiography and hemodynamic measurements after tail-vein injection of saline, cFibro, CSCs^{GFP}, or CSCs$^{GFP/TK}$ in ISO+5-FU-treated rats and after administration of GCV to CSCs$^{GFP/TK}$ animals. *$p < 0.05$ versus CTRL.

(D) Quantification of c-kit^{pos}eCSC and GFP^{pos}CMs. *$p < 0.05$ versus CTRL; §$p < 0.05$ versus groups at 2 months; #$p < 0.05$ versus groups at 3 months.

(E) Representative confocal microscopy of c-kit^{pos} (white) CSCs^{GFP} (green) in the myocardium of rats with ISO+5FU cardiomyopathy rescued by CSC^{GFP} injection.

(F) Flow cytometric analysis of c-kit^{pos}CSCs^{GFP} isolated 2 months after tail vein injection.

(G and H) Confocal microscopy of c-kit^{pos}CSCs^{GFP}-derived CMs in situ and following isolation at 3 months after tail-vein injection. Scale bar, 20 μm.

All data are mean ± SD. See also Figures S7 and S8 and Table S5.

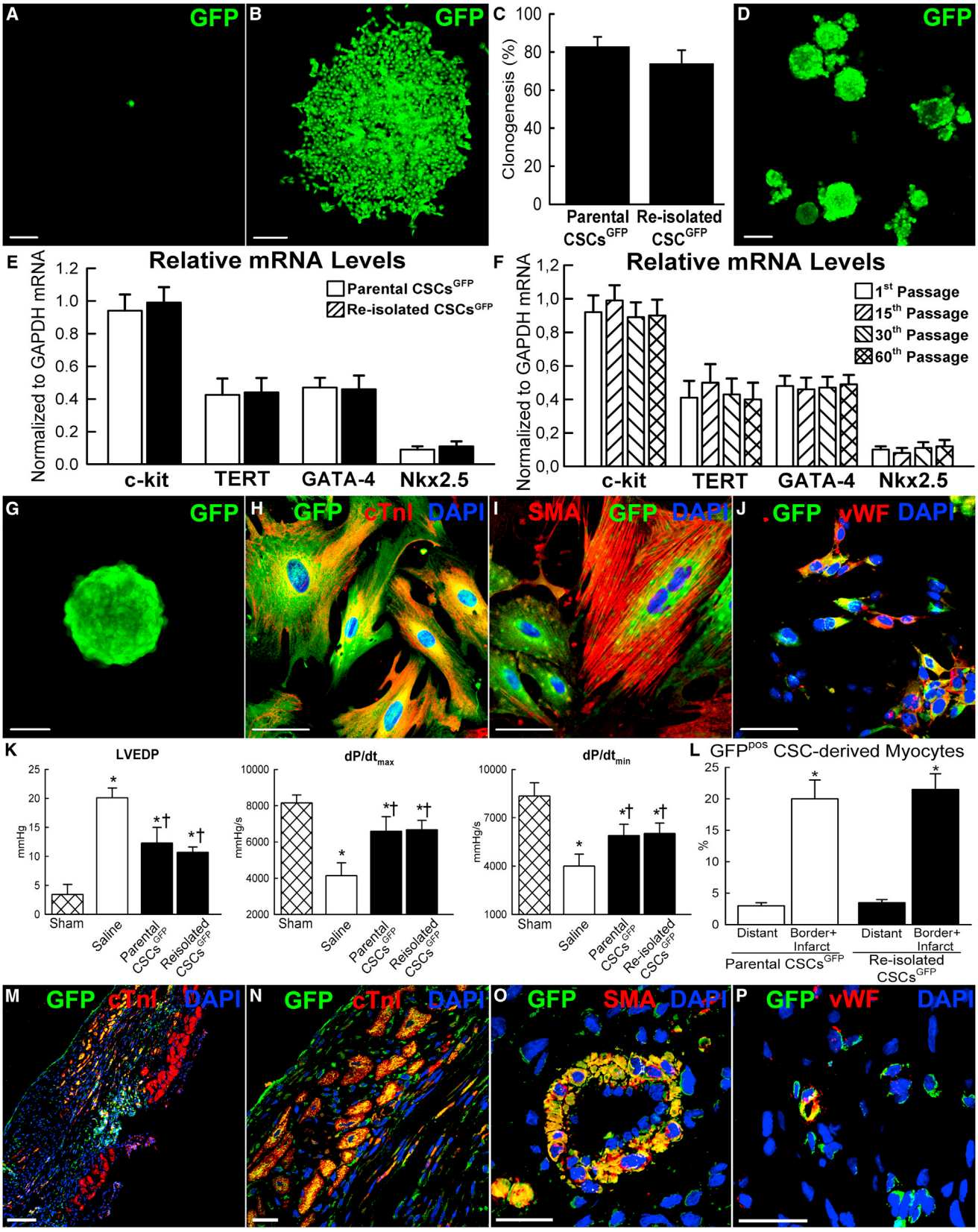

(legend on next page)

chimerism; Figures 6D, 6F, and S7). These CSC^{GFP} chimeric hearts had complete restoration of ventricular volumes and function (Figures 6B, 6C, and S7 and Table S5) with ~8% GFP^{pos} CMs (Figure 6D), indicating that they are the progeny of the transplanted cells. These data, in addition to highlighting the homing and regenerative capacity of the CSCs, also point to these cells as one of the cell targets of the in vivo direct reprogramming protocols for myocardial regeneration using retroviral vectors encoding CM-determining genes (Qian et al., 2012; Song et al., 2012).

To rule out that cell fusion was the source of the new GFP^{pos} CMs in the CSCs^{GFP}-transplanted animals, cloned male CSCs^{GFP} were injected into female rat recipients with ISO+5FU cardiomyopathy as above. X and Y chromosomes were identified in GFP^{pos} cells and their CM progeny. None of the GFP^{pos} cells had more than one X chromosome, ruling out cell fusion as the source of the GFP^{pos} CMs (Figure S7). Furthermore, cloned c-kit^{pos}eCSCs from MerCreMer mice transduced with red fluorescence protein were injected into RYP mice with ISO+5FU cardiomyopathy and chased with tamoxifen before sacrifice. We could not detect any red-labeled eCSC-derived CMs expressing EYFP, which, if present, would identify cell fusion (Figure S7).

Histological and functional results identical to the injection of exogenous CSCs^{GFP} were obtained in ISO+5FU-induced cardiomyopathic animals by injection of GFP^{pos}TK^{pos}CSCs (CSCs$^{GFP/TK}$) (Figures 6B–6D and S7 and Table S5). At 56 days (~2 months), additional animals with ISO+5-FU cardiomyopathy rescued by exogenous CSCs^{GFP} or CSCs$^{GFP/TK}$ were treated with either saline or GCV for 2 weeks and sacrificed at 84 days (~3 months). At this time point, CSCs^{GFP} and CSCs$^{GFP/TK}$ rats treated with saline showed a fully reconstituted eCSC pool together with myocardial regeneration and repair (Figures 6D, 6G, and S7). Myocardial immunohistochemistry was corroborated at the single-cell level, quantifying isolated rod-shaped GFP^{pos} CMs by immunocytochemistry and FACS (Figures 6H and S8). CSC-derived GFP^{pos} CMs were still mostly mononucleated but had a size comparable to pre-existing CMs, indicating that the maturation of newly generated CMs is completed in 2 months (Figures 6G and S8). Furthermore, CSC^{GFP}-derived CMs expressed cardiac transcription factors and contractile genes with mRNA levels comparable with normal adult CMs (Figure S8).

GCV treatment did not cause any histological or functional adverse effects to the rats in the ISO+5-FU+CSC^{GFP} group. In contrast, GCV treatment of ISO+5-FU+CSCs$^{GFP/TK}$ group activated the programmed suicide of CSCs$^{GFP/TK}$ and their progeny, which caused a dramatic reversal of all the recovered cellular and functional parameters (Figures 6D and S7). At 3 months, the myocardium was devoid of CSCs$^{GFP/TK}$ and of GFP^{pos} CM progeny (Figure 6D), which was accompanied by pathologic remodeling, ventricular chamber dilation, and hemodynamic deterioration to levels of overt cardiac failure (Figure 6D and Table S5).

Finally, the reported "bystander effect" of GCV (Yoon et al., 2010) was ruled out by several lines of evidence. First, GCV at a concentration sufficient to kill the CSCs$^{GFP/TK}$ cultured with adult rat ventricular CMs in a 10:1 ratio does not affect survival of the latter (Figure S8). Second, early time points after GCV administration showed death of only CSCs$^{GFP/TK}$ and CSCs$^{GFP/TK}$-derived CMs and not of the larger spared GFP^{neg} neighboring CMs (data not shown). Third, GCV-derived metabolites effectively kill cycling cells, whereas noncycling terminally differentiated cells are naturally resistant to it.

Transplanted CSCs^{GFP} Reisolated after Having Regenerated the Damaged Myocardium Retain Tissue-Specific Stem Cell Properties

To test whether, after transplantation, some of the engrafted GFP^{pos} cells remain bona fide eCSCs, cells dissociated from the hearts with ISO+5-FU cardiomyopathy rescued by CSCs^{GFP} were FACS sorted for c-kit and GFP. These c-kit^{pos}CSCs^{GFP} reisolated from the transplanted hearts exhibited a phenotype indistinguishable from the parental c-kit^{pos}CSC^{GFP} clone originally transplanted (Figure 7). They were clonogenic, self-renewing, formed typical cardiospheres, and differentiated into CMs, endothelial, and smooth-muscle cells in vitro (Figures 7A–7J). A clone of the reisolated c-kit^{pos}CSC^{GFP}, when transplanted back into rats with ISO+5FU cardiomyopathy, proved indistinguishable from the primary parental clone in their efficiency to replenish the depleted eCSC and CM-pool and reverse the severe cardiac dysfunction (Figure S9). Furthermore, when these reisolated cells were transplanted into rats with acute myocardial infarction, they repopulated the ischemic myocardium with new GFP^{pos} CMs and vascular cells, leading to improved LV function (Figures 7K–7Q).

DISCUSSION

The results presented here demonstrate that c-kit^{pos}eCSCs behave as true resident, endogenous stem cells, which are necessary and sufficient for myocardial repair and cellular

Figure 7. Reisolated CSCs^{GFP} Retain Tissue-Specific Stem Cell Properties

(A–D) CSC^{GFP} isolated from cell chimeric hearts produces single-cell-derived clones (A–C) and cardiospheres (D) with similar efficiency to the clonal parental CSC^{GFP}. Scale bar, 100 μm.

(E and F) qRT-PCR transcript profile (E) and profile over passage number (F) of reisolated CSC^{GFP}.

(G–J) Immunocytochemistry identifies reisolated CSC^{GFP} cardiospheres (G), which differentiated into CMs (H; cTnI), smooth muscle (I; SMA), and endothelial (J; vWF) cells in vitro. Scale bar, 50 μm.

(K and L) LV function measurements (K) and quantification of new GFP^{pos} CMs (L) following injection of reisolated clonal CSC^{GFP} into the infarcted rat heart (K, *$p < 0.05$ versus Sham and $^{\dagger}p < 0.05$ versus saline) (L, *$p < 0.05$ versus Distant).

(M–P) Confocal microscopy of new GFP^{pos} CMs (cTnI; M and N), arteries (SMA; O), and capillaries (vWF; P) in the border/infarct area. Scale bar, 100 μm (M) and 20 μm (N–P).

All data are mean ± SD. See also Figure S9.

homeostasis. These results, however, do not rule out the participation of other cardiac stem-cell-like populations (Oh et al., 2003; Chong et al., 2011; Smart et al., 2011) or minor contributions by other cells (Senyo et al., 2013). Because the c-kit/cre lentivirus strategy labeled approximately half of the c-kit^{pos} eCSCs in the LV (Figure 3), these results cannot determine whether the fraction of newly generated EYFP^{neg} CMs was not labeled because of the lentivirus inefficiency in vivo or because some of them are the progeny of c-kit^{neg} stem and progenitor cells. Nonetheless, the replacement of the eCSC cohort by the progeny of a single CSC convincingly favors the first alternative.

It is generally accepted that, in healthy adult tissue, most stem cells are quiescent and if they cycle they do so very slowly, providing just enough transient amplifying cells to maintain tissue homeostasis (Orford and Scadden, 2008). In contrast, the quiescent stem cells in response to injury are rapidly activated, multiply, and differentiate to replace the cells lost. In the healthy adult myocardium, >90% of the c-kit^{pos}eCSCs are quiescent (G0) (Figure 1). In response to diffuse ISO injury, most eCSCs enter the cell cycle, replicate, and commit to the myocardial cell lineages (Figure 1), including CMs (Figure 3). Once the ISO-induced cell loss and cardiac failure have been corrected by the regenerated cells, the number of activated eCSCs diminishes progressively with a concomitant increase of the quiescent cohort (Figure 1). Thus, the return to myocardial homeostasis is accompanied by the return of activated eCSCs to their quiescent state. This roundtrip from dormancy to activation and back to quiescence has been suggested for other self-renewing organs (Wilson et al., 2008). This toggling between eCSC cycling states might just highlight the important role of these cells in the homeostasis of a tissue essential for organismic survival. Understanding the mechanisms by which cycling eCSCs return to quiescence has clinical implications to exploit the regenerative potential of these cells.

The efficiency of some adult stem cells, such as HSCs and eCSCs, to specifically home to and nest into their tissue of origin is dependent on tissue damage together with depletion of the resident stem cells. This is so because the number of tissue niches appears to be limited and nonexpandable (Czechowicz et al., 2007). Here, we show that the injured myocardium provides a milieu that supports the homing, nesting, survival, and differentiation of the CSCs (Figure 4). However, if after injury the eCSCs are left in the tissue, despite the very effective cardiac homing of the transplanted CSC^{GFP}, only a very small number succeed in long-term nesting in the myocardium. This behavior contrasts with a host myocardium that has been depleted of most eCSCs prior to transplantation (Figures 5 and 6). Then the empty niches are very efficiently occupied by the CSCs^{GFP} transplanted through the systemic circulation, which not only survive but differentiate into the four main myocardial cell types and reconstitute the resident eCSC pool (Figure 6). The sturdiness of the CSC homing, engraftment, and regenerative properties after many passages in culture and cloning (Figure 7) contrasts with the reported loss of engraftment of ex-vivo-expanded HSCs (Guenechea et al., 1999) and skeletal muscle satellite cells (Montarras et al., 2005). Therefore, this robust homing of the eCSCs could be exploited to replace the stem cell population of the myocardium by noninvasive means, as clinically implemented now for the bone marrow.

The HSCs are the best-understood adult stem cells and have become the standard for most adult stem cell biology. Unfortunately, solid tissues have serious experimental limitations over the bone marrow, in which it is possible to transplant a single genetically tagged HSC and follow its progeny in the host (Rossi et al., 2008). That no such feat is possible in solid tissues has hampered most attempts to define the role of tissue-specific stem cells in the regenerative process. So far there is no report of replacing the ablated stem cells with genetically tagged exogenous cells in solid tissues. Such replacement is required to produce a chimeric tissue whose regeneration can be shown to be dependent on the transplanted cells. In the myocardium, the best approximation to the HSC paradigm is transplantation of the progeny of a single cell. The high degree of cell chimerism obtained by transplantation of cloned CSCs^{GFP} and CSC$^{TK/GFP}$ shows that the progeny of a single CSC can reconstitute the 5-FU ablated eCSC cohort and generate a cell chimeric heart with new cardiomyocytes and vascular cells, thereby restoring cardiac function. That the cellular and functional regeneration of the ISO-damaged myocardium is due to the transplanted CSCs is clearly shown by the rapid deterioration of cardiac function when these cells and their progeny are selectively killed by the GCV (Figure 6).

The data presented here support the conclusion that the eCSCs are necessary and sufficient for anatomical and functional regeneration of the adult mammalian myocardium.

EXPERIMENTAL PROCEDURES

Animals

Diffuse myocardial damage was induced by a single injection (s.c.) of ISO to rats (5 mg kg^{-1}) or mice (200 mg kg^{-1}). To ablate cycling cells, including eCSCs, after ISO-damage, 5-FU (Sigma) was administered (10 mg kg^{-1}) for four cycles of 5 days each, starting at the third day post-ISO injection. Mer-CreMer mice were kindly provided by Drs. Tammie Bishop and Ludwig Thierfelder. ZEG and RYP mice were purchased at Jackson Laboratory. GCV was administered (i.p.) at the dose of 50 mg kg^{-1} twice daily for 14 days.

Lenti c-kit/cre

The c-kit/cre construct was generated starting from a construct encoding the EGFP gene under the c-kit promoter (Cairns et al., 2003) by replacing EGFP with the CRE gene.

Statistical Analysis

Data are reported as mean ± SD. Significance was determined by ANOVA. The Bonferroni post hoc method was used to locate the differences. Significance was set at $p < 0.05$.

ACCESSION NUMBERS

The GEO accession number for the microarray data reported in this paper is GSE49318.

SUPPLEMENTAL INFORMATION

Supplemental Information includes Extended Experimental Procedures, nine figures, and seven tables and can be found with this article online at http://dx.doi.org/10.1016/j.cell.2013.07.039.

ACKNOWLEDGMENTS

This work was supported by grants from the CARE-MI FP7 (Health-F5-2010-242038), Endostem FP7 (Health F5-2010-241440) large-scale collaborative projects, Marie Curie International Reintegration FP7 Grant (PIRG02-GA-2007-224853), FIRB-Futuro-in-Ricerca (RBFR081CCS), Italian Ministry of Health (GR-2008-1142673), Associazione Italiana per la Ricerca sul Cancro (AIRC) MFAG-2008, and Istituto Superiore di Sanità (RF-CAL-2008-1261292). We sincerely thank Tammie Bishop (University of Oxford) and Ludwig Thierfelder (Max-Delbrueck Center for Molecular Medicine) for providing the MerCreMer mice; Edmondo Battista and Filippo Causa (Center for Advanced Biomaterials for Healthcare, Italian Institute of Technology and Interdisciplinary Research Center on Biomaterials, University Federico II) for their technical help in manufacturing the fibrin-based PEGylated hydrogel; and Aurora Nocera and Emilia Dora Giovannone (CIS of Genomics and Molecular Pathology, Magna Graecia University) for their excellent technical help in cardiomyocyte FACS sorting.

Received: December 14, 2012
Revised: May 3, 2013
Accepted: July 26, 2013
Published: August 15, 2013

REFERENCES

Akashi, Y.J., Goldstein, D.S., Barbaro, G., and Ueyama, T. (2008). Takotsubo cardiomyopathy: a new form of acute, reversible heart failure. Circulation *118*, 2754–2762.

Askari, A.T., Unzek, S., Popovic, Z.B., Goldman, C.K., Forudi, F., Kiedrowski, M., Rovner, A., Ellis, S.G., Thomas, J.D., DiCorleto, P.E., et al. (2003). Effect of stromal-cell-derived factor 1 on stem-cell homing and tissue regeneration in ischaemic cardiomyopathy. Lancet *362*, 697–703.

Beltrami, A.P., Barlucchi, L., Torella, D., Baker, M., Limana, F., Chimenti, S., Kasahara, H., Rota, M., Musso, E., Urbanek, K., et al. (2003). Adult cardiac stem cells are multipotent and support myocardial regeneration. Cell *114*, 763–776.

Bergmann, O., Bhardwaj, R.D., Bernard, S., Zdunek, S., Barnabé-Heider, F., Walsh, S., Zupicich, J., Alkass, K., Buchholz, B.A., Druid, H., et al. (2009). Evidence for cardiomyocyte renewal in humans. Science *324*, 98–102.

Cairns, L.A., Moroni, E., Levantini, E., Giorgetti, A., Klinger, F.G., Ronzoni, S., Tatangelo, L., Tiveron, C., De Felici, M., Dolci, S., et al. (2003). Kit regulatory elements required for expression in developing hematopoietic and germ cell lineages. Blood *102*, 3954–3962.

Chong, J.J., Chandrakanthan, V., Xaymardan, M., Asli, N.S., Li, J., Ahmed, I., Heffernan, C., Menon, M.K., Scarlett, C.J., Rashidianfar, A., et al. (2011). Adult cardiac-resident MSC-like stem cells with a proepicardial origin. Cell Stem Cell *9*, 527–540.

Czechowicz, A., Kraft, D., Weissman, I.L., and Bhattacharya, D. (2007). Efficient transplantation via antibody-based clearance of hematopoietic stem cell niches. Science *318*, 1296–1299.

Dong, F., Harvey, J., Finan, A., Weber, K., Agarwal, U., and Penn, M.S. (2012). Myocardial CXCR4 expression is required for mesenchymal stem cell mediated repair following acute myocardial infarction. Circulation *126*, 314–324.

Ellison, G.M., Torella, D., Karakikes, I., and Nadal-Ginard, B. (2007a). Myocyte death and renewal: modern concepts of cardiac cellular homeostasis. Nat. Clin. Pract. Cardiovasc. Med. *4*(*Suppl 1*), S52–S59.

Ellison, G.M., Torella, D., Karakikes, I., Purushothaman, S., Curcio, A., Gasparri, C., Indolfi, C., Cable, N.T., Goldspink, D.F., and Nadal-Ginard, B. (2007b). Acute beta-adrenergic overload produces myocyte damage through calcium leakage from the ryanodine receptor 2 but spares cardiac stem cells. J. Biol. Chem. *282*, 11397–11409.

Ellison, G.M., Galuppo, V., Vicinanza, C., Aquila, I., Waring, C.D., Leone, A., Indolfi, C., and Torella, D. (2010). Cardiac stem and progenitor cell identification: different markers for the same cell? Front Biosci (Schol Ed) *2*, 641–652.

Ellison, G.M., Torella, D., Dellegrottaglie, S., Perez-Martinez, C., Perez de Prado, A., Vicinanza, C., Purushothaman, S., Galuppo, V., Iaconetti, C., Waring, C.D., et al. (2011). Endogenous cardiac stem cell activation by insulin-like growth factor-1/hepatocyte growth factor intracoronary injection fosters survival and regeneration of the infarcted pig heart. J. Am. Coll. Cardiol. *58*, 977–986.

Guenechea, G., Segovia, J.C., Albella, B., Lamana, M., Ramírez, M., Regidor, C., Fernández, M.N., and Bueren, J.A. (1999). Delayed engraftment of nonobese diabetic/severe combined immunodeficient mice transplanted with ex vivo-expanded human CD34(+) cord blood cells. Blood *93*, 1097–1105.

Hsieh, P.C., Segers, V.F., Davis, M.E., MacGillivray, C., Gannon, J., Molkentin, J.D., Robbins, J., and Lee, R.T. (2007). Evidence from a genetic fate-mapping study that stem cells refresh adult mammalian cardiomyocytes after injury. Nat. Med. *13*, 970–974.

Jesty, S.A., Steffey, M.A., Lee, F.K., Breitbach, M., Hesse, M., Reining, S., Lee, J.C., Doran, R.M., Nikitin, A.Y., Fleischmann, B.K., and Kotlikoff, M.I. (2012). c-kit+ precursors support postinfarction myogenesis in the neonatal, but not adult, heart. Proc. Natl. Acad. Sci. USA *109*, 13380–13385.

Kajstura, J., Rota, M., Cappetta, D., Ogórek, B., Arranto, C., Bai, Y., Ferreira-Martins, J., Signore, S., Sanada, F., Matsuda, A., et al. (2012). Cardiomyogenesis in the aging and failing human heart. Circulation *126*, 1869–1881.

Loffredo, F.S., Steinhauser, M.L., Gannon, J., and Lee, R.T. (2011). Bone marrow-derived cell therapy stimulates endogenous cardiomyocyte progenitors and promotes cardiac repair. Cell Stem Cell *8*, 389–398.

Lompré, A.M., Nadal-Ginard, B., and Mahdavi, V. (1984). Expression of the cardiac ventricular alpha- and beta-myosin heavy chain genes is developmentally and hormonally regulated. J. Biol. Chem. *259*, 6437–6446.

Montarras, D., Morgan, J., Collins, C., Relaix, F., Zaffran, S., Cumano, A., Partridge, T., and Buckingham, M. (2005). Direct isolation of satellite cells for skeletal muscle regeneration. Science *309*, 2064–2067.

Oh, H., Bradfute, S.B., Gallardo, T.D., Nakamura, T., Gaussin, V., Mishina, Y., Pocius, J., Michael, L.H., Behringer, R.R., Garry, D.J., et al. (2003). Cardiac progenitor cells from adult myocardium: homing, differentiation, and fusion after infarction. Proc. Natl. Acad. Sci. USA *100*, 12313–12318.

Orford, K.W., and Scadden, D.T. (2008). Deconstructing stem cell self-renewal: genetic insights into cell-cycle regulation. Nat. Rev. Genet. *9*, 115–128.

Orlic, D., Kajstura, J., Chimenti, S., Jakoniuk, I., Anderson, S.M., Li, B., Pickel, J., McKay, R., Nadal-Ginard, B., Bodine, D.M., et al. (2001). Bone marrow cells regenerate infarcted myocardium. Nature *410*, 701–705.

Qian, L., Huang, Y., Spencer, C.I., Foley, A., Vedantham, V., Liu, L., Conway, S.J., Fu, J.D., and Srivastava, D. (2012). In vivo reprogramming of murine cardiac fibroblasts into induced cardiomyocytes. Nature *485*, 593–598.

Rossi, D.J., Jamieson, C.H., and Weissman, I.L. (2008). Stems cells and the pathways to aging and cancer. Cell *132*, 681–696.

Sata, M., Saiura, A., Kunisato, A., Tojo, A., Okada, S., Tokuhisa, T., Hirai, H., Makuuchi, M., Hirata, Y., and Nagai, R. (2002). Hematopoietic stem cells differentiate into vascular cells that participate in the pathogenesis of atherosclerosis. Nat. Med. *8*, 403–409.

Schneider, J.W., Gu, W., Zhu, L., Mahdavi, V., and Nadal-Ginard, B. (1994). Reversal of terminal differentiation mediated by p107 in Rb-/- muscle cells. Science *264*, 1467–1471.

Senyo, S.E., Steinhauser, M.L., Pizzimenti, C.L., Yang, V.K., Cai, L., Wang, M., Wu, T.D., Guerquin-Kern, J.L., Lechene, C.P., and Lee, R.T. (2013). Mammalian heart renewal by pre-existing cardiomyocytes. Nature *493*, 433–436.

Smart, N., Bollini, S., Dubé, K.N., Vieira, J.M., Zhou, B., Davidson, S., Yellon, D., Riegler, J., Price, A.N., Lythgoe, M.F., et al. (2011). De novo cardiomyocytes from within the activated adult heart after injury. Nature *474*, 640–644.

Song, K., Nam, Y.J., Luo, X., Qi, X., Tan, W., Huang, G.N., Acharya, A., Smith, C.L., Tallquist, M.D., Neilson, E.G., et al. (2012). Heart repair by reprogramming non-myocytes with cardiac transcription factors. Nature *485*, 599–604.

Takeuchi, J.K., and Bruneau, B.G. (2009). Directed transdifferentiation of mouse mesoderm to heart tissue by defined factors. Nature *459*, 708–711.

Tallini, Y.N., Greene, K.S., Craven, M., Spealman, A., Breitbach, M., Smith, J., Fisher, P.J., Steffey, M., Hesse, M., Doran, R.M., et al. (2009). c-kit expression identifies cardiovascular precursors in the neonatal heart. Proc. Natl. Acad. Sci. USA *106*, 1808–1813.

Torella, D., Ellison, G.M., Karakikes, I., and Nadal-Ginard, B. (2007). Resident cardiac stem cells. Cell. Mol. Life Sci. *64*, 661–673.

Vincent, S.D., and Buckingham, M.E. (2010). How to make a heart: the origin and regulation of cardiac progenitor cells. Curr. Top. Dev. Biol. *90*, 1–41.

Waring, C.D., Vicinanza, C., Papalamprou, A., Smith, A.J., Purushothaman, S., Goldspink, D.F., Nadal-Ginard, B., Torella, D., and Ellison, G.M. (2012). The adult heart responds to increased workload with physiologic hypertrophy, cardiac stem cell activation, and new myocyte formation. Eur. Heart J.. http://dx.doi.org/10.1093/eurheartj/ehs338.

Weissman, I.L. (2000). Translating stem and progenitor cell biology to the clinic: barriers and opportunities. Science *287*, 1442–1446.

Wilson, A., Laurenti, E., Oser, G., van der Wath, R.C., Blanco-Bose, W., Jaworski, M., Offner, S., Dunant, C.F., Eshkind, L., Bockamp, E., et al. (2008). Hematopoietic stem cells reversibly switch from dormancy to self-renewal during homeostasis and repair. Cell *135*, 1118–1129.

Yoon, C.H., Koyanagi, M., Iekushi, K., Seeger, F., Urbich, C., Zeiher, A.M., and Dimmeler, S. (2010). Mechanism of improved cardiac function after bone marrow mononuclear cell therapy: role of cardiovascular lineage commitment. Circulation *121*, 2001–2011.

Zaruba, M.M., Soonpaa, M., Reuter, S., and Field, L.J. (2010). Cardiomyogenic potential of C-kit(+)-expressing cells derived from neonatal and adult mouse hearts. Circulation *121*, 1992–2000.

Zhang, G., Wang, X., Wang, Z., Zhang, J., and Suggs, L. (2006). A PEGylated fibrin patch for mesenchymal stem cell delivery. Tissue Eng. *12*, 9–19.